Molecular Determinants of Inactivation within the I-II Linker of α1E (Ca_V2.3) Calcium Channels

L. Berrou, G. Bernatchez, and L. Parent
Department of Physiology, Membrane Transport Research Group, Université de Montréal, Montréal, Québec H3C 3J7 Canada

ABSTRACT Voltage-dependent inactivation of Ca_V2.3 channels was investigated using point mutations in the β-subunit-binding site (AID) of the I-II linker. The quintuple mutant α1E N381K + R384L + A385D + D388T + K389Q (NRADK-KLDTQ) inactivated like the wild-type α1E. In contrast, mutations of α1E at position R378 (position 5 of AID) into negatively charged residues Glu (E) or Asp (D) significantly slowed inactivation kinetics and shifted the voltage dependence of inactivation to more positive voltages. When co-injected with β3, R378E inactivated with $\tau_{inact} = 538 \pm 54$ ms ($n = 14$) as compared with 74 ± 4 ms ($n = 21$) for α1E ($p < 0.001$) with a mid-potential of inactivation $E_{0.5} = -44 \pm 2$ mV ($n = 10$) for R378E as compared with $E_{0.5} = -64 \pm 3$ mV ($n = 9$) for α1E. A series of mutations at position R378 suggest that positively charged residues could promote voltage-dependent inactivation. R378K behaved like the wild-type α1E whereas R378Q displayed intermediate inactivation kinetics. The reverse mutation E462R in the L-type α1C (Ca_V1.2) produced channels with inactivation properties comparable to α1E R378E. Hence, position 5 of the AID motif in the I-II linker could play a significant role in the inactivation of Ca_V1.2 and Ca_V2.3 channels.

INTRODUCTION

The influx of calcium through neuronal voltage-gated Ca^{2+} channels regulates a wide range of cellular processes, including neurotransmitter release, activation of Ca^{2+}-dependent enzymes and second messenger cascades, gene regulation, and proliferation. To this date, molecular cloning has identified the primary structures for 10 distinct calcium channel α_1 subunits: α1S (Ca_V1.1), α1C (Ca_V1.2), α1D (Ca_V1.3), and α1F (Ca_V1.4) encode L-type channels; α1A (Ca_V2.1) encodes both P- and Q-type channels; α1B (Ca_V2.2) defines N-type channels; α1G (Ca_V3.1), α1H (Ca_V3.2), and α1I (Ca_V3.3) form T-type channels (Cribbs et al., 1998, 2000; Lee et al., 1999a; Monteil et al., 2000; Ertel et al., 2000) and α1E (Ca_V2.3) probably encodes a component of the resistant current identified in some neuronal preparations (Randall and Tsien, 1997; Piedras-Renteria and Tsien, 1998; Saegusa et al., 2000).

Calcium channel inactivation is a critical determinant of the temporal precision of calcium signals and serves to prevent long-term increases in intracellular calcium levels. In the L-type α1C channel, inactivation proceeds mostly in response to localized elevation of intracellular Ca^{2+} providing negative Ca^{2+} feedback (deLeon et al., 1995; Bernatchez et al., 1998). The dominant Ca^{2+} sensor for such Ca^{2+}-dependent inactivation in α1C and α1A Ca^{2+} channels has recently been identified as calmodulin, which appears to be constitutively tethered to the channel complex (Qin et al., 1999; Zuhlke et al., 1999; Peterson et al., 1999; Lee et al., 1999b). This Ca^{2+} sensor induces channel inactivation by Ca^{2+}-dependent calmodulin binding to an IQ-like motif situated on the carboxyl tail of α1C (Peterson et al., 2000).

Fast and voltage-dependent inactivation appears to be a key mechanism by which other Ca^{2+} channels achieve regulation of internal calcium levels. The molecular mechanisms for voltage-dependent inactivation in Ca^{2+} channel proteins are incompletely understood. The importance of the I-II linker in Ca^{2+} channel inactivation has, however, recently emerged in various studies. Point mutations and chimeras in that region were shown to modify inactivation kinetics in α1A (Herlitze et al., 1997) and α1C channels (Adams and Tanabe, 1997). Overexpression of mRNA coding for the I-II linker from α1A, but not for the III-IV linker, was shown to speed up inactivation of wild-type α1A/β2a in *Xenopus* oocytes (Cens et al., 1999). A chimeric channel containing the I-II linker from α1E accelerated the inactivation kinetics of α1C (Stotz et al., 2000). Conversely we have also recently observed that the I-II linker from α1C conferred slower inactivation kinetics to α1E (unpublished data). Hence, the I-II linker of HVA α1 subunits appears a likely candidate for an inactivating blocking particle in an updated version of the hinged-lid mechanism observed in Na^+ channels. In this model, most β-subunits would regulate Ca^{2+} channel inactivation kinetics by priming the I-II linker into a conformation more favorable to inactivation.

The I-II linker contains many crucial regulatory sites in Ca^{2+} channels. The I-II linker contains the high-affinity β-subunit-binding site AID (alpha-1 subunit interaction domain) that was first identified by protein overlay (Pragnell et al., 1994) and was shown to participate in β-subunit regulation (DeWaard and Campbell, 1995; Gerster et al., 1999; DeWaard et al., 1996). Mutations within the AID motif in α1A perturbed β binding (Pragnell et al., 1994). There are secondary binding sites between the cytoplasmic β- and the α1-subunits on the N-terminus for α1B (Ste-

Received for publication 29 June 2000 and in final form 5 October 2000.
Address reprint requests to Dr. L. Parent, Département de Physiologie, Membrane Transport Research Group, Université de Montréal, P.O. Box 6128, Downtown Station, Montréal, Québec, H3C 3J7 Canada. Tel.: 514-343-6673; Fax: 514-343-7146; E-mail: lucie.parent@umontreal.ca.

0006-3495/01/01/215/14 $2.00

phens et al., 2000) and α1A (Walker et al., 1999) and on the C-terminus for α1E (Tareilus et al., 1997), but AID appears to be universally present in all non-T-type α1-subunits (Perez-Reyes et al., 1998). The AID binding site is composed of QQXEXXLXGYXXWIXXXE, and a single substitution at the conserved Y (Tyr) position could disrupt plasma membrane targeting of the α1-subunit without, however, affecting the β-subunit-induced modulation of whole-cell and single-channel currents (Gerster et al., 1999). The I-II linker of the α1-subunit contains an endoplasmic reticulum retention signal that is antagonized by the β-subunit (Bichet et al., 2000). Last, the I-II linker was also shown to interact with G-protein $\beta\gamma$-subunit (DeWaard et al., 1997; Dolphin, 1998) in a competitive fashion with β-subunits (Campbell et al., 1995).

Recent studies have strongly suggested a critical role for the I-II linker, and more precisely for the β-subunit-binding site (AID) in the inactivation of voltage-dependent Ca^{2+} channels (VDCCs) (Page et al., 1997; Herlitze et al., 1997). Indeed, conversion of the AID motif from QQIE*R*E to QQIE*E*E slowed inactivation of α1A channels as well as shifting its voltage dependence of inactivation to more positive potentials (Herlitze et al., 1997).

Point mutations E462R in α1C and its counterpart R387E in α1E channels were herein shown to significantly influence both the kinetics and the voltage dependence of inactivation. Furthermore, a quintuple mutant made in the same region, α1E N381K + R384L + A385D + D388T + K389Q, failed to affect either kinetics or voltage dependence of inactivation. Hence, along with containing the G-protein regulation site and the retention signal, the I-II loop in Ca^{2+} channel α1-subunits may thus underlie three important modulatory influences in VDCCs.

MATERIALS AND METHODS

Recombinant DNA techniques

Standard methods of plasmid DNA preparation were used (Sambrook et al., 1989). cDNAs coding for wild-type rabbit α1C (GenBank X15539) and β3 (Genbank M88751) were kindly donated by Dr. E. Perez-Reyes. The wild-type human α1E (GenBank L27745) was a gift from Dr. T. Schneider. The rat brain α2bδ-subunit was provided by Dr. T. P. Snutch. For the α1C mutants, a site *XhoI* was first engineered by polymerase chain reaction into α1C at position 1530 nt in the I-II linker, roughly 40 residues downstream to the β-subunit-binding site on the α1-subunit (AID). This is a nonsilent mutation creating a Gly-to-Arg mutation at this position. The resulting α1C (*XhoI*) channel, however, displayed inactivation and activation kinetics similar to the wild-type α1C (see Figs. 2 and 7). For point mutations, repeat I of α1E and α1C were respectively subcloned in Topo XL (Invitrogen, Carlsbad, CA) for conveniently using the Unique Site Elimination method (Pharmacia Biotech) developed by Deng and Nickoloff (1992) with *DraI*/*HpaI* selection. Constructs were verified by restriction mapping, and recombinant clones were screened by double-stranded sequence analysis of the entire ligated cassette. The nucleotide sequence of the mutated region was determined by the dideoxy chain termination method using either single- or double-stranded plasmid DNA (T7 Sequenase v 2.0, Amersham Pharmacia Biotech) in house or sent out for automatic sequencing by BioST (Lachine, Québec, Canada). cDNA constructs for wild-type and mutated α1-subunits were linearized at the 3′ end by *HindIII* digestion whereas the rat brain β3-subunit was digested by *NotI*. Run-off transcripts were prepared using methylated cap analog $m^7G(5')ppp(5')G$ and T7 RNA polymerase with the mMessage mMachine transcription kit (Ambion, Austin, TX). The final cRNA products were resuspended in DEPC-treated H_2O and stored at −80°C. The integrity of the final product and the absence of degraded RNA was determined by a denaturing agarose gel stained with ethidium bromide.

Functional expression of wild-type and mutant channels

Oocytes were obtained from female *Xenopus laevis* clawed frog (Nasco, Fort Atkinson, WI) as described previously (Parent et al., 1995, 1997; Parent and Gopalakrishnan, 1995; Bernatchez et al., 1998). Individual oocytes free of follicular cells were obtained after 30–40 min of incubation in a calcium-free solution (in mM: 82.5 NaCl, 2.5 KCl, 1 $MgCl_2$, 5 Hepes, pH 7.6) containing 2 mg/ml collagenase (Gibco, Burlington, Ontario, Canada). Forty-six nanoliters of a solution containing between 35 and 50 ng of cRNA coding for the wild-type or mutated α1-subunit was injected 16 h later into stage V and VI oocytes. The cRNA concentration of the α1-subunit was generally adjusted to yield whole-cell peak currents in the 1–5-μA range; hence RNA concentration coding for the α1E wild-type and mutant channels was established at the lowest end of this range whereas α1C wild-type and α1C E462R channels were measured after injection with the highest concentration possible. When specified, cRNA coding for rat brain α2bδ (Williams et al., 1992) and rat brain β3 (Castellano et al., 1993) were co-injected with the α1-subunit at a 3:1:1 weight ratio. Oocytes were incubated at 19°C in a Barth's solution (in mM): 100 NaCl, 2 KCl, 1.8 $CaCl_2$, 1 $MgCl_2$, 5 HEPES, 2.5 pyruvic acid, 100 U/ml penicillin, 50 μg/ml gentamicin, pH 7.6. The inactivation properties of each mutant channel herein described was studied in a minimum of three different oocyte batches to account for the typical expression variability encountered from batch to batch. Furthermore, the corresponding wild-type channel (α1E in most cases) was systematically injected under the same experimental conditions every time a new mutant was analyzed, thus insuring that the mutant behavior was not caused by some aberrant properties (such as higher level of endogenous β-subunits) (Lacerda et al., 1994; Tareilus et al., 1997) of this particular batch of oocytes. Hence the properties of the wild-type α1E channel were analyzed in seven different oocyte batches for the current study.

Electrophysiological recordings in oocytes

Wild-type and mutant channels were screened at room temperature for macroscopic barium current 4 to 7 days after RNA injection using a two-electrode voltage-clamp amplifier (OC-725C, Warner Instruments, Hamden, CT) as described earlier (Parent et al., 1995, 1997). Voltage and current electrodes were slightly broken under the microscope to decrease the electrode resistance to 0.5–1.5-MΩ tip resistance and were filled with 3 M KCl, 1 mM EGTA, 10 mM HEPES (pH 7.4). Oocytes were first impaled in a modified Ringer solution (in mM): 96 NaOH, 2 KOH, 1.8 $CaCl_2$, 1 $MgCl_2$, 10 HEPES titrated to pH 7.4 with methanesulfonic acid CH_3SO_3H (MeS). The bath was then perfused with the 10 mM Ba^{2+} solution (in mM: 10 $Ba(OH)_2$, 110 NaOH, 1 KOH, 20 Hepes titrated to pH 7.3 with MeS). To minimize kinetic contamination by the endogenous Ca^{2+}-activated Cl^- current, oocytes were injected with 18.4 nl of a 50 mM EGTA solution (Sigma, St. Louis, MO) 0.5–2 h before the experiments. Oocytes were superfused by gravity flow at a rate of 2 ml/min, which was fast enough to allow complete chamber fluid exchange within 30 s. Experiments were performed at room temperature (20–22°C).

Data acquisition and analysis

PClamp software, Clampex 6.02 and Clampfit 6.02 (Axon Instruments, Foster City, CA), was used for on-line data acquisition and analysis. Unless stated otherwise, data were sampled at 10 kHz and low pass filtered at 5 kHz using the amplifier built-in filter. For all recordings, a series of voltage pulses were applied from a holding potential of −80 mV at a frequency of 0.2 Hz from −40 to +60 mV. Isochronal inactivation data (h_∞ or h_{inf}) were obtained from tail currents generated at the end of a 5-s prepulse (Parent et al., 1995). Tail current amplitudes were estimated using the function Analyze in Clampfit 6.0 from the peak current arising during the first 10 ms after the capacitive transient (20 data points). Each of these currents was then normalized to the maximum current obtained before the prepulse voltage (i/i_{max}) and was plotted against the prepulse voltage. For the isochronal inactivation figures, data points represent the mean of $n \geq 3$ and were fitted to the Boltzmann Eq. 1:

$$\frac{i}{i_{max}} = 1 - \frac{1 - Y_o}{1 + \left\{\exp - \frac{zF}{RT}(V_m - E_{0.5})\right\}} \quad (1)$$

Pooled data points (mean ± SEM) were fitted to Eq. 1 using user-defined functions and the fitting algorithms provided by Origin 6.0 (Microcal Software, Northampton, MA) analysis software. Eq. 1 accounts for the fraction of non-inactivating current with $E_{0.5}$, mid-point potential; z, slope parameter; Y_0, fraction of non-inactivating current; V_m, the prepulse potential; and RT/F with their usual meanings. The fitting process generated values estimating errors on the given fit values.

Activation parameters were estimated from the mean *I-V* curves obtained for each channel combination. The *I-V* relationships were normalized to the maximum amplitude and were fitted to the Boltzmann Eq. 2:

$$\frac{i}{i_{max}} = \frac{1}{1 + \left\{\exp - \frac{zF}{RT}(V_m - E_{0.5})\right\}} \quad (2)$$

$E_{0.5}$ is the potential for 50% activation, z is slope parameter, V_m is the test potential, and RT/F have their usual meanings. The fitting process generated values estimating errors on the given fit values.

As the number of exponential functions needed to account for the inactivation process varied between α1C and α1E channels, inactivation kinetics were quantified using r300 values, that is, the ratio of the whole-cell current remaining at the end of a 300-ms pulse. As inactivation kinetics can vary with current density, comparisons between constructs and mutants were generally restricted to whole-cell currents lower than 5 μA as much as possible. Furthermore, this range of current densities made it easier to voltage clamp the oocyte uniformly, thus decreasing the possibility of series resistance artifacts contaminating the current kinetics data.

Capacitive transients were erased for clarity in the final figures. Statistical analyses and Student *t*-test were performed using the fitting routines provided by Origin 5.0 and 6.0 (Microcal Software).

RESULTS

Recent studies have strongly suggested a critical role for the I-II linker and, more precisely, for the β-subunit-binding site (AID) in the inactivation of voltage-dependent Ca^{2+} channels (VDCCs) (Page et al., 1997; Herlitze et al., 1997; Adams and Tanabe, 1997; Cens et al., 1999; Stotz et al., 2000). Some unpublished results from our lab obtained using α1E/α1C chimeras also point toward the high-affinity β-subunit-binding site in the I-II of the α1-subunit (AID) as an important determinant of voltage-dependent inactivation in α1E channels (unpublished data). As the AID motif is conserved in all non-T-type α1-subunits, this observation suggests a role for nonconserved residues present in the AID domain. It is composed of a short stretch of 18 residues located in the 5′ end of the I-II linker. Fig. 1 shows the consensus sequence QQXEXXLXGYXXWIXXXE for the β-subunit-binding site in the six gene families α1S, α1C, α1D, α1A, α1B, and α1E. Identical residues are shown in bold. Of the nine nonconserved residues, positions 3 and 6 of the AID motif involve conservative mutation from an Iso (I) to a Leu (L) and from a Glu (E) to an Asp (D); position 17 is actually a conserved Ala (A) residue between α1E and α1C. Position 5 is occupied by an Arg (R) that is strictly conserved in non-L-type and is replaced by a Glu (E) in L-type. Hence we undertook a detailed mutagenesis study of the six nonconservative residues in the AID motif of α1E with R378, N381, R384, A385, D388, or K389 alone or in combination.

Residue R378 is critical for α1E (Ca_V2.3) fast inactivation kinetics

Fig. 2 shows a family of whole-cell current recordings obtained in the presence of 10 mM Ba^{2+} for the wild-type α1E, triple-mutant N381K + R384L + A385D, quintuple-mutant N381K + R384L + A385D + D388T + K389Q, and point mutations K389E and R378E expressed in *Xenopus* oocytes on the α2bδ and β3 auxiliary subunit background. Current traces recorded under the same conditions for the modified α1C (*XhoI*) channel (used to produce the α1C E462R mutant) are shown for comparison. The β3-subunit was the chosen subunit as it triggers inactivation mostly from the closed state in neuronal Ca^{2+} channels as opposed to β2a that favors inactivation from the open state (Patil et al., 1998). The quintuple-mutant NRADK-KLDTQ includes five of the six nonconserved residues between α1E and α1C in the AID motif. As seen, the triple-mutant NRA-KLD (positions 8, 11, and 12 of AID) and the quintuple-mutant NRADK-KLDTQ (positions 8, 11, 12, 15, and 16 of AID) inactivated like the wild-type α1E channel. Similar data were obtained with the quadruple-mutant NRAK-KLDQ (positions 8, 11, 12, and 16 of AID; results not shown). For instance, 95 ± 1% (n = 21) of the α1E whole-cell currents were inactivated at the end of a 300-ms pulse to 0 mV, which is identical to 96 ± 1% (n = 3) for NRA-KLD, 96 ± 1% (n = 4) for NRAK-KLDQ, and 96 ± 2% (n = 5) for NRADK-KLDTQ. In contrast, a single point mutation at position R378 (position 5 in AID) produced whole-cell currents with significantly slower inactivation kinetics with only 72 ± 4% (n = 13) of the R378E currents being inactivated under the same conditions. Mutation of the positively charged Lys residue at position 389 (position 16 in AID) to a negatively charged Glu (K to E) produced an intermediary inactivation phenotype with 85 ± 2% (n =

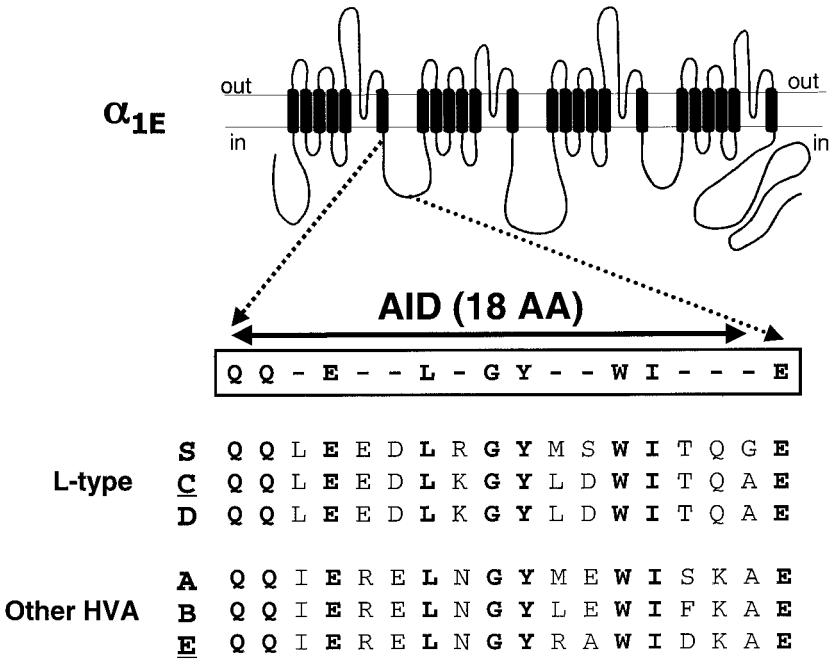

FIGURE 1 Predicted secondary structure for the human brain α1E ($Ca_V2.3$) channel with the four homologous repeats and the N and the C termini facing the cytoplasm. The β-subunit-binding site on the α1 subunit (AID) is located within 20 residues of the IS6 transmembrane segment. The consensus sequence for the AID motif (QQxExxLxGYxxWIxxxE) is shown with conserved residues in bold letters. Non-conserved residues are represented by slashes (-) on the figure. The amino acid alignment for L-type (α1S ($Ca_V1.1$), α1C ($Ca_V1.2$), and α1D ($Ca_V1.3$)) and non-L-type (α1A ($Ca_V2.1$), α1B ($Ca_V2.2$), and α1E ($Ca_V2.3$)) Ca^{2+} channels within this region is displayed enlarged. Of the nine "x" sites, positions 3 and 6 of the AID involve conservative mutation from an Iso (I) to a Leu (L) and from a Glu (E) to an Asp (D); position 17 is actually a conserved Ala (A) residue between α1E and α1C. Position 5 of AID is occupied by an Arg (R) that is strictly conserved in non-L-type and is replaced by a Glu (E) in L-type. These residues correspond to R378 in α1E and E462 in α1C.

15) of the currents inactivated at the end of a pulse to 0 mV. It should be noted that the milder K389Q mutation achieved within the quadruple and the quintuple mutants produced no significant effect on inactivation (Fig. 2). These rates of inactivation remained significantly faster than the rates observed for α1C (*XhoI*), for only 29 ± 3% (n = 6) of these currents were inactivated under the same conditions. Current density did not appear to play a significant role in modulating inactivation kinetics in this series of experiments (Table 1). Whole-cell current density was lower for the fast inactivating mutant α1E NRA-KLD whereas the largest currents were generally recorded for α1E R378E.

Inactivation kinetics were computed using r300 ratios (Peterson et al., 2000), i.e., the fraction of whole-cell currents remaining at the end of a 300-ms pulse (Fig. 3 *A*). As seen, the rate of inactivation increased slightly with depo-

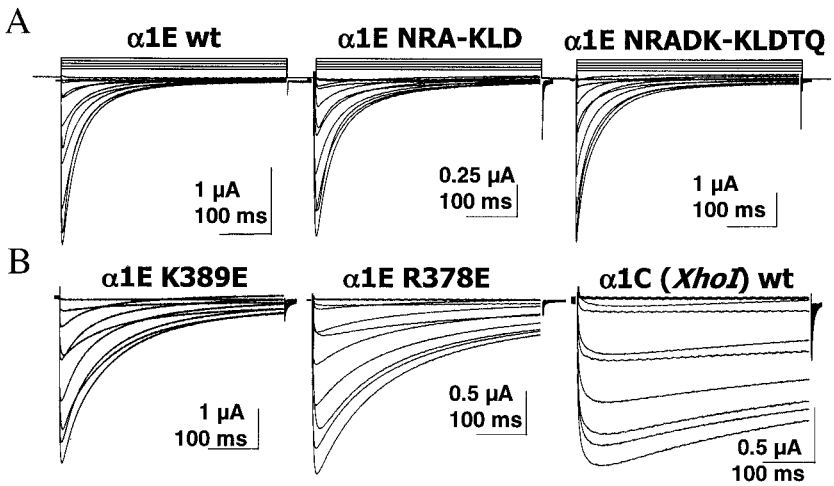

FIGURE 2 The α1E wt, α1E N381K + R384L + A385D (NRA), and α1E N381K + R384L + A385D + D388T + K389Q (NRADK) (*A*) and α1E K389E, α1E R378E, and α1C (*XhoI*) (*B*) were expressed in *Xenopus* oocytes in the presence of α2bδ and β3 subunits. Whole-cell currents were recorded using the two-electrode voltage-clamp technique in the presence of 10 mM Ba^{2+} after injection of EGTA. Holding potential was −80 mV. Oocytes were pulsed from −40 mV to +60 mV using 10-mV steps for 450 ms. Capacitive transients were erased for the first millisecond after the voltage step. All mutants tested expressed significant whole-cell currents. Inactivation kinetics were slower in mutants K389E and R378E. Mutant and wild-type channels displayed similar activation properties (Table 1). Whole-cell currents peaked at −4 ± 2 mV (n = 7) for α1E; −3 ± 3 mV (n = 3) for NRA-KLD; −5 ± 3 mV (n = 4) for NRAK-KLDQ; −3 ± 3 mV (n = 3) for NRADK-KLDTQ; −3 ± 2 mV (n = 9) for α1E R378E, and −4 ± 2 mV (n = 9) for α1C (*XhoI*).

TABLE 1 Biophysical properties of α1E ($Ca_V2.3$) and α1C ($Ca_V1.2$) channels and mutants

Channels expressed with α2bδ/β3	Inactivation (5 s)		Activation		
	$E_{0.5}$ (mV)	z	$E_{0.5}$ (mV)	z	Peak I_{Ba} (μA)
α1E wt	−64 ± 3 (9)	3.5 ± 0.4	−18 ± 2 (9)	6.1 ± 0.4	−3.7 ± 1.3 (21)
α1E NRA-KLD	−68 ± 2 (7)	2.8 ± 0.5	−15 ± 2 (7)	6.0 ± 0.5	−1.9 ± 0.4 (7)
NRAK-KLDQ	−64 ± 3 (4)	3.1 ± 0.5	−11 ± 2 (4)	5.7 ± 0.4	−3.6 ± 1.4 (4)
NRADK-KLDTQ	−60 ± 2 (3)	2.8 ± 0.6	−15 ± 1 (3)	5.8 ± 0.2	−2.4 ± 1.2 (5)
α1E K389E	−60 ± 3 (5)	2.2 ± 0.7	−14 ± 4 (9)	5.4 ± 0.2	−4.1 ± 1.1 (15)
α1E R378K	−63 ± 2 (5)	3.2 ± 0.3	−14 ± 3 (5)	4.8 ± 0.3	−2.7 ± 1.5 (7)
α1E R378A	−51 ± 2 (6)*	3.3 ± 0.2	−21 ± 5 (6)	5.1 ± 0.3	−2.6 ± 0.6 (7)
α1E R378Q	−51 ± 2 (8)*	3.1 ± 0.2	−12 ± 3 (8)	4.8 ± 0.3	−3.1 ± 0.5 (8)
α1E R378G	−52 ± 2 (10)*	2.9 ± 0.4	−19 ± 4 (11)	6.1 ± 0.2	−3.8 ± 1.0 (11)
α1E R378D	−46 ± 3 (11)†	2.7 ± 0.3	−16 ± 3 (9)	6.2 ± 0.5	−3.5 ± 0.7 (14)
α1E R378E	−44 ± 2 (10)†	2.3 ± 0.5	−14 ± 3 (14)	5.5 ± 0.3	−4.6 ± 1.7 (14)
α1C E462R	−31 ± 2 (12)†	4.2 ± 0.2	−14 ± 4 (8)	6.7 ± 0.5	−2.0 ± 0.4 (12)
α1C (*XhoI*)	−23 ± 3 (8)‡	3.4 ± 0.4	−13 ± 5 (8)	9 ± 2	−3.3 ± 0.3 (9)
α1C wt	−20 ± 4 (12)‡	3.1 ± 0.4	−11 ± 3 (7)	10 ± 2	−3.9 ± 0.5 (17)

Biophysical parameters of α1E and α1C wild-type (wt) and mutant channels expressed in *Xenopus* oocytes in the presence of α2bδ and β3 subunits. Whole-cell currents were measured in 10 mM Ba^{2+} throughout. The voltage dependence of inactivation was determined after 5-s pulses from −100 to +50 mV as shown on Fig. 6. Relative currents were fitted to Boltzmann Eq. 1. Activation data were estimated from the mean *I-V* relationships and fitted to Boltzmann Eq. 2. Peak I_{Ba} was determined from *I-V* relationships for the corresponding experiments. The data are shown with the mean ± SEM and the number of samples (n) appears in parentheses. Significance of difference between α1E and other channels is given by $^{*}p < 0.05$, $^{\dagger}p < 0.005$, and $^{\ddagger}p < 0.001$.

larization for the α1E wild-type and mutant channels. α1E NRA-KLD, NRAK-KLDQ (results not shown), and NRADK-KLDTQ mutants behaved like the wild-type α1E at all potentials tested. In contrast, the r300 ratios were significantly higher for α1E R378E ($p < 0.002$) and α1E K389E ($p < 0.05$) as compared with α1E. Altogether, these results suggest that fast inactivation in α1E depends on the nature of residues at positions 5 and 16 of the AID.

The activation potentials were estimated from the mean peak current-voltage relationships (Fig. 3 *B*). Activation potentials were similar for NRA-KLD, NRADK-KLDTQ (results not shown), and α1E wt with $E_{0.5}$ values around −17 mV and slightly more positive for the quadruple-mutant NRAK-KLDQ with $E_{0.5} = -11$ mV (see Table 1 for the exact values). Whereas inactivation kinetics were significantly slower for α1E K389E and R378E, both mutants were found to activate in a range of potentials not significantly different than α1E wt (Table 1).

Position 5 in the AID motif influences the voltage dependence of α1E ($Ca_V2.3$) inactivation

If inactivation kinetics reflect the rate of transition to the inactivated state(s), the isochronal inactivation data provide the voltage range where channels are most likely to inactivate. The voltage dependence of inactivation was assessed from the relative tail currents measured after a series of 5-s depolarizations. Fig. 3 *C* shows a family of isochronal inactivation data for the wild-type α1E channel, NRA-KLD, NRAK-KLDQ (results not shown), NRADK-KLDTQ, K389E, R378E, and α1C wt. Mid-potentials of inactivation ($E_{0.5}$) were estimated from Boltzmann fits (Eq. 1). The voltage dependence of the isochronal inactivation for the first four mutant channels were comparable, with $E_{0.5}$ varying from −60 mV (NRADK and K389E) to −68 mV (NRA). These values were not significantly different from the $E_{0.5}$ of −64 mV for wild-type α1E channels (Table 1). Hence, most mutants in the AID motif inactivated in the same voltage range as the wild-type α1E channel. Only mutant R378E experienced a significant shift in its voltage dependence of inactivation toward more positive potentials as compared with the wild-type α1E with a $E_{0.5} = -44$ mV. This change in the voltage dependence of inactivation of α1E R378E occurred without any significant shift in the voltage dependence of activation (Table 1).

Structural requirements for fast inactivation kinetics at position 378 of α1E ($Ca_V2.3$)

Of the six nonconserved residues in the AID motif, only R378 was shown to affect both the kinetics and voltage dependence of inactivation. A series of point mutations was thus undertaken to evaluate the importance of the charge, the volume, and the hydrophilicity of the residue 378 in the α1E inactivation process. Fig. 4 shows the family of whole-cell Ba^{2+} current traces of mutants R378K, R378Q, R378A, R378G, R378D, and R378E after expression in *Xenopus* oocytes. Mutant α1E R378K displayed the fastest inactivation kinetics closely followed by R378A and R378Q. At −10 mV, the rate of inactivation ranked as follows (from the fastest to the slowest) α1E wt ≈ R378K ≈ R378A > R378Q ≫ R378G ≈ R378D ≈ R378E as seen by the r300 analysis shown in Fig. 5 *A*. This ranking remained true at voltages between −10 and +20 mV, although inactivation

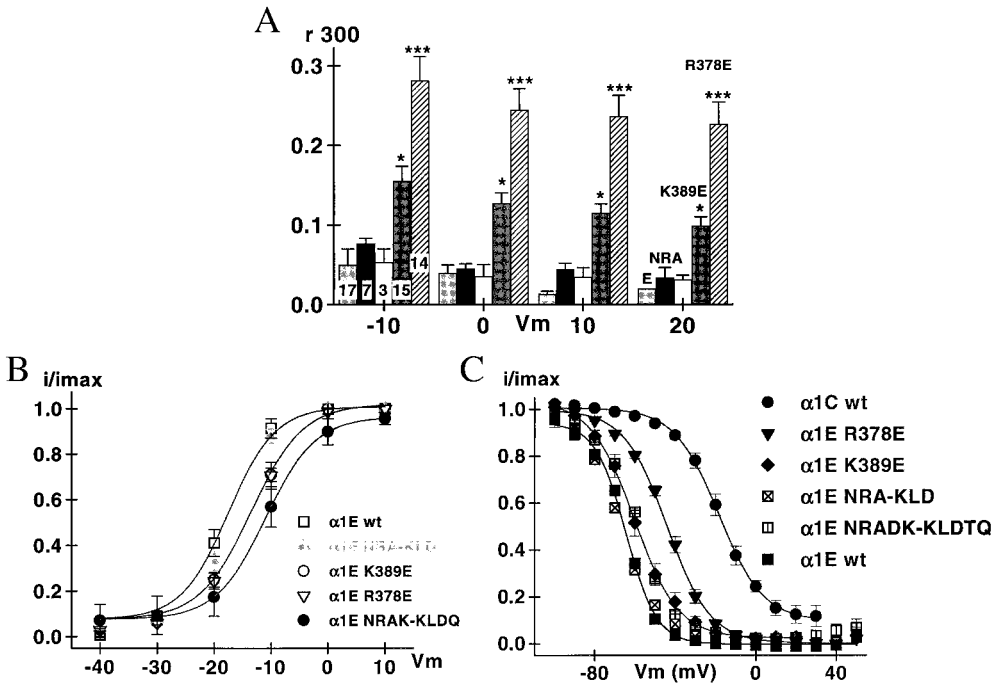

FIGURE 3 (*A*) The mean r300 ratios (the fraction of the whole-cell current remaining at the end of a 300-ms pulse) are shown ± SEM at four voltages from −10 to +20 mV for α1E wt (*light gray*), α1E N381K + R384L + A385D (NRA) (*black*), α1E N381K + R384L + A385D + D388T + K389Q (NRADK) (*white*), α1E K389E (*dark gray*), and α1E R378E (*hatched*) from left to right as measured in 10 mM Ba^{2+}. The numbers on the columns refer to the numbers of experiments (*n*) used for statistical analysis. The r300 ratios varied from 0.05 ± 0.02 at −10 mV to 0.02 ± 0 ($n = 17$) at +20 mV for α1E and from 0.05 ± 0.02 at −10 mV to 0.03 ± 0.01 ($n = 14$) at +20 mV for NRADK-KLDTQ, NRAK-KLDQ, and NRA-KLD mutants when the data are pooled together. In contrast, r300 ratios were significantly different between α1E wt and α1E K389E ($p < 0.01$) varying from 0.16 ± 0.02 at −10 mV to 0.10 ± 0.01 ($n = 15$) at +20 mV for α1E K389E. The r300 ratios were also significantly different between α1E wt and α1E R378E ($p < 0.002$) with values from 0.33 ± 0.04 at −10 mV to 0.27 ± 0.03 ($n = 14$) at +20 mV for R378E. (*B*) Activation potentials were estimated from the mean normalized current-voltage relationships. The relative data points were plotted against the test voltage and were fitted to Boltzmann Eq. 2. The activation potentials were comparable for α1E wt, NRA-KLD, NRAK-KLDQ, NRADK-KLDTQ (results not shown), α1E K389E, and α1E R378E. The fit values are given in Table 1. (*C*) The voltage dependence of inactivation was measured after a 5-s conditioning prepulse applied between −100 and +50 mV. The protocol is shown in detail in Fig. 6. The voltage dependence of inactivation was not significantly different for α1E wt, NRA-KLD, NRAK-KLDQ (results not shown), NRADK-KLDTQ, and α1E K389E with $E_{0.5}$ varying from −68 to −60 mV. In contrast, the mid-potential of inactivation for R378E was −44 ± 2 mV ($n = 10$). Fit values are shown in Table 1.

kinetics tended to get faster with membrane depolarization especially for mutants R378Q, R378G, R378D, and R378E. The rate of R378K inactivation was comparable to α1E at −10 and 0 mV but differed slightly at higher membrane potential as its inactivation kinetics remained relatively insensitive to depolarization. For R378Q, the r300 ratio was significantly ($p < 0.05$) different from R378K at −10 mV, but these differences were attenuated at +20 mV. The r300 ratios for the neutral residue R378A were noticeably similar to R378K and to the wild-type α1E channel at all membrane potentials. R378A, a small and neutral residue, behaved like R378K, but R378G, which is also a small and neutral residue, behaved like negatively charged mutants R378D and R378E. Altogether, these results suggest that positively charged residues at this position may stimulate faster inactivation kinetics whereas negatively charged residues could trigger slower rates of inactivation. However, the effects of the neutral residues (A, Q, and G) cannot be simply explained in terms of either charge or size. Furthermore, none of the point mutations cause the α1E channel to inactivate in the same voltage range as the wild-type α1C.

The slower inactivation kinetics for R378 mutants were not correlated with any apparent change in their activation kinetics. Furthermore, the activation potentials $E_{0.5}$ for mutants R378E, R378D, R378G, R378A, and R378K were comparable to the $E_{0.5}$ for the wild-type α1E channel. Only R378Q appeared to activate at membrane potentials slightly more positive than the wild-type α1E channel. Hence, the reported shifts in the inactivation potentials for the R378 mutants were probably not linked to changes in whole-cell activation properties.

Mutations at position 378 affect voltage-dependent inactivation of the human α1E ($Ca_V2.3$)

The next series of experiments was undertaken to evaluate whether the charge of the side-chain at position 378 played

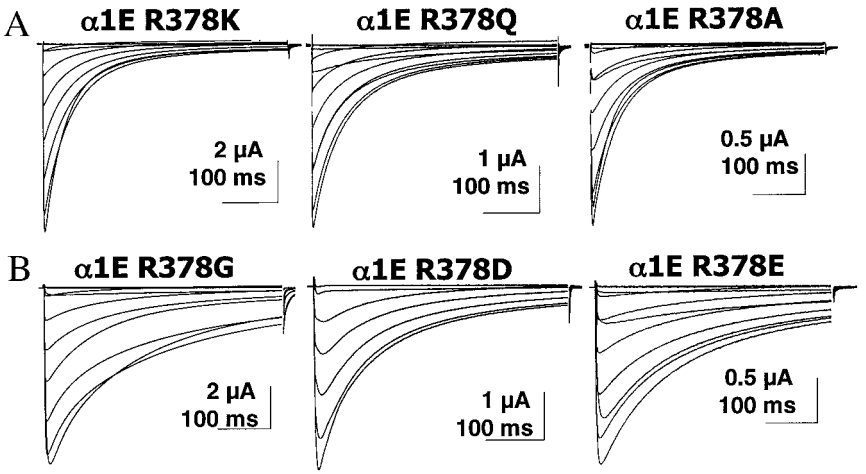

FIGURE 4 Mutants α1E R378K, α1E R378Q, and α1E R378A (*A*) and α1E R378G, α1E R378D, and α1E R378E (*B*) were expressed in *Xenopus* oocytes in the presence of α2bδ and β3 subunits. Current traces were obtained in the presence of 10 mM Ba^{2+} after injection of EGTA. Holding potential was −80 mV. Oocytes were pulsed from −40 mV to +60 mV using 10-mV steps for 450 ms. Capacitive transients were erased for the first millisecond after the voltage step. All mutants tested expressed significant whole-cell currents. Inactivation kinetics appeared slower in mutants R378G, R378D, and R378E.

a role in the voltage range where α1E channels inactivate. Fig. 6 shows the isochronal inactivation data measured after 5-s pulses were applied from −100 mV to voltages between −100 and +50 mV. Typical current traces are shown for the wild-type α1E and mutants R378K, R378Q, and R378E with an example of the voltage protocol used. The inactivation data for α1E R378K superimposed quite closely with the inactivation data points for the wild-type α1E (Table 1). In contrast, inactivation data points are shifted to the right for mutants α1E R378A, R378Q, R378G, R378D, and R378E and lay halfway between α1C and α1E. Mid-potentials of inactivation ranged from $E_{0.5} = -52$ mV for R378G to $E_{0.5} = -44$ mV for R378E. As seen above, the shifts in the voltage dependence of inactivation were not accompanied by any significant shift in the activation potentials (Table 1).

The reverse mutation E462R triggers faster inactivation kinetics in α1C ($Ca_V1.2$)

The alignment shown in Fig. 1 pointed out that the positively charged arginine (R) residue in non-L-type Ca^{2+} channels is replaced by a glutamate (E) residue that is conserved in all L-type channels. Replacement of residue 378 with the corresponding residue of α1C was shown to slow inactivation kinetics and shift the voltage dependence of inactivation. The reverse mutation of E to R in the brain α1C channel has already been examined and was actually shown to speed up inactivation of the slower α1C channel (Herlitze et al., 1997). To compare the inactivation properties of α1E R378E and α1C E462R under our experimental conditions, we performed the α1C E462R mutation and expressed it in *Xenopus* oocytes. Fig. 7 *A* shows whole-cell current traces for α1E, α1C E462R, α1E R378E, and α1C that were scaled and superimposed at membrane potentials between −10 and +10 mV. As seen on Fig. 7 *B*, α1C E462R and α1E R378E inactivated with a similar time course that turned out to be intermediary between the fast α1E and the slow α1C channel at all voltages with r300 ratios of ~0.3 in both cases. In contrast, r300 ratios for α1C wt and α1C (*XhoI*) are higher with values of ~0.7. As seen, the inactivation kinetics for the modified α1C (*XhoI*) channel used for making α1C E462R were compiled and were found to be similar to the wild-type α1C channel. Hence, neither point mutation in α1E or α1C could completely reverse the inactivation phenotype to the opposite wild-type channel. As inactivation kinetics of α1C are exquisitely sensitive upon the current density, it should be pointed out that the current density for α1C E462R was in average smaller than for α1C (*XhoI*), ruling out current density as a critical factor for the faster inactivation kinetics (Table 1).

The voltage dependence of inactivation was next studied for mutant α1C E462R (5-s prepulses) and compared with α1E, α1E R378E, and α1C (*XhoI*) (Fig. 7 *C*). As compared with the α1C (*XhoI*) channel, the inactivation data points for α1C E462R were shifted to the left by −10 mV, but they remained significantly more positive than the inactivation curve for α1E R378E. Furthermore, the slope of the fit was much steeper for α1C E462R than for any other mutant tested in this study.

Given the fact that the I-II linker could also be involved in calcium-dependent inactivation (Adams and Tanabe, 1997), the inactivation kinetics of α1C E462R were also measured in the presence of 10 mM Ca^{2+}. Like the wild-type α1C, α1C E462R was found to inactivate significantly faster in the presence of Ca^{2+} ions. For instance, the r300 ratios went from 0.39 ± 0.04 ($n = 6$) in Ba^{2+} to 0.14 ± 0.01 ($n = 3$) in Ca^{2+} at −10 mV and from 0.26 ± 0.02 ($n = 6$) in Ba^{2+} to 0.014 ± 0.001 ($n = 3$) in Ca^{2+} at +20 mV. These numbers compare well with the r300 ratios for α1C under the same Ca^{2+} conditions with 0.13 ± 0.03 at −10 mV and 0.14 ± 0.01 at +20 mV ($n = 8$). This result indicates that mutations in the AID motif that disrupt voltage-dependent inactivation may not necessarily impair calcium-dependent inactivation, and further suggests that AID may not be the blocking particle common to both voltage-

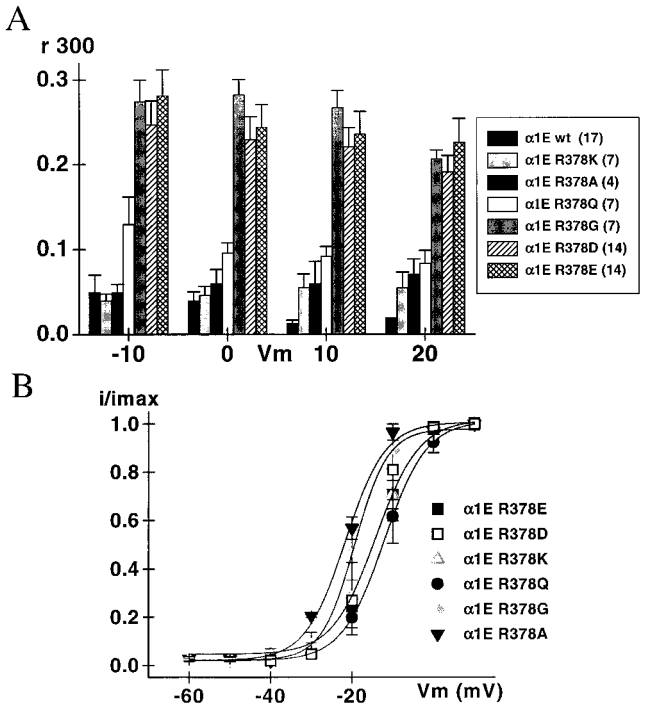

FIGURE 5 (*A*). Whole-cell currents obtained in the presence of 10 mM Ba^{2+}. The mean r300 ratios (the fraction of the whole-cell current remaining at the end of a 300-ms pulse) are shown ± SEM at four voltages from −10 to +20 mV for α1E wt (*black*), α1E R378K (*light gray*), α1E R378A (*dark gray*), α1E R378Q (*white*), α1E R378G (*gray*), α1E R378D (*hatched*), and α1E R378E (*cross-hatched*) from left to right. At −10 mV, the r300 ratios for α1E R378K and α1E R378A were not significantly different from α1E wt whereas those for α1E R378Q were different at $p < 0.05$ and those for α1E R378G, α1E R378D, and α1E R378E were significantly different at $p < 0.002$. The r300 ratios went from 0.04 ± 0.01 at −10 mV and 0.05 ± 0.02 at +20 mV ($n = 7$) for R378K, from 0.05 ± 0.01 at −10 mV to 0.06 ± 0.02 at +20 mV ($n = 4$) for R378A, from 0.13 ± 0.03 at −10 mV to 0.08 ± 0.02 at +20 mV ($n = 7$) for R378Q, from 0.27 ± 0.03 at −10 mV and 0.21 ± 0.01 at + 20 mV ($n = 7$) for R378G, from 0.25 ± 0.03 at −10 mV to 0.19 ± 0.02 at +20 mV ($n = 14$) for R378D, and from 0.28 ± 0.03 at −10 mV to 0.23 ± 0.03 at +20 mV ($n = 14$) for R378E as compared with 0.05 ± 0.02 at −10 mV and 0.02 ± 0.01 at +20 mV ($n = 17$) for α1E. The number (n) of experiments is shown in parentheses. (*B*) Activation potentials were estimated from the mean normalized current-voltage relationships. The relative data points were plotted against the test voltage and were fitted to Boltzmann Eq. 2. The activation potentials were comparable for all mutants although they increased slightly from α1E R378A ≈ α1E R378G ≈ α1E wt < α1E R378K ≈ α1E R378D ≈ α1E R378E < α1E R378Q. Table 1 contains the actual fit values.

and calcium-dependent inactivation mechanisms (Cens et al., 1999).

β-Subunit regulation is preserved in α1E R378E and α1C E462R channel mutants

As β-subunits are known to modulate the inactivation kinetics of the α1-subunit and to bind to the AID site (Pragnell et al., 1994), the next series of experiments was undertaken to examine the possibility that the altered inactivation kinetics of α1E R378E and α1C E462R were secondary to a modification in the coupling between β3 and α1-subunits as all previous experiments were performed in the presence of a full complement of auxiliary α2bδ- and β3-subunits. The objectives were twofold: 1) to explore whether modifications in nonconserved residues in AID could influence β-subunit modulation of the inactivation kinetics and 2) to evaluate whether the changes in the inactivation kinetics were intrinsically determined by the α1-subunit. Mutant α1E R378E and α1C E462R were expressed in *Xenopus* oocytes in the presence (α2bδ/β3) and in the absence of β3 with only α2bδ as ancillary subunit (Fig. 8). Whole-cell currents were recorded in the presence of 10 mM Ba^{2+} under strictly paired conditions (same day of expression, same oocyte batch) to minimize nonspecific effects. The presence of β3 induced a leftward shift of the peak voltage by −10 mV for both α1C E462R and α1E R378E (results not shown), which is similar to what has been reported before for the wild-type channels (Parent et al., 1997). The voltage dependence of inactivation estimated from isochronal measurements at 5 s was shifted to the left in the presence of β3 with $E_{0.5} = -11 \pm 2$ mV ($n = 4$) (−β3) and $E_{0.5} = -26 \pm 2$ mV ($n = 6$) (+β3) for α1C E462R and $E_{0.5} = -26 \pm 1$ mV ($n = 3$) (−β3) and $E_{0.5} = -44 \pm 1$ mV ($n = 3$) (+β3) for α1E R378E (results not shown). It thus appears that the mutants retained some modulation by the β3-subunit despite structural rearrangements in the main β-subunit-binding site.

The time courses of inactivation for α1C E462R and α1E R378E remained comparable to each other whether it was measured in the absence (left panel) or in the presence of β3 (right panel) under all conditions except at −10 mV in the absence of β3 as it can be inferred from the r300 ratio analysis (lower left panel). Moreover, the inactivation kinetics of both mutants remained significantly slower than α1E ($p < 0.005$) under all conditions. The inactivation kinetics of α1C/α2bδ were not reported as its expression in oocytes never rose above background currents. Co-injection with the β3-subunit led to an apparent increase in inactivation kinetics for both mutants, which was confirmed by the r300 analysis. Hence, the inactivation kinetics remained similar for α1E R378E and α1C E462R in the absence of β3.

DISCUSSION

Position R378 in the AID motif is critical in α1E ($Ca_V2.3$) inactivation

In this study, the molecular determinants of voltage-dependent inactivation in the α1E Ca^{2+} channel were investigated following mutations within the high-affinity β-subunit-binding site (AID) of the I-II linker. The AID motif is composed of a stretch of 18 amino acids located about at the 5′ end of the I-II linker that reads QQXEXXLXGYX-

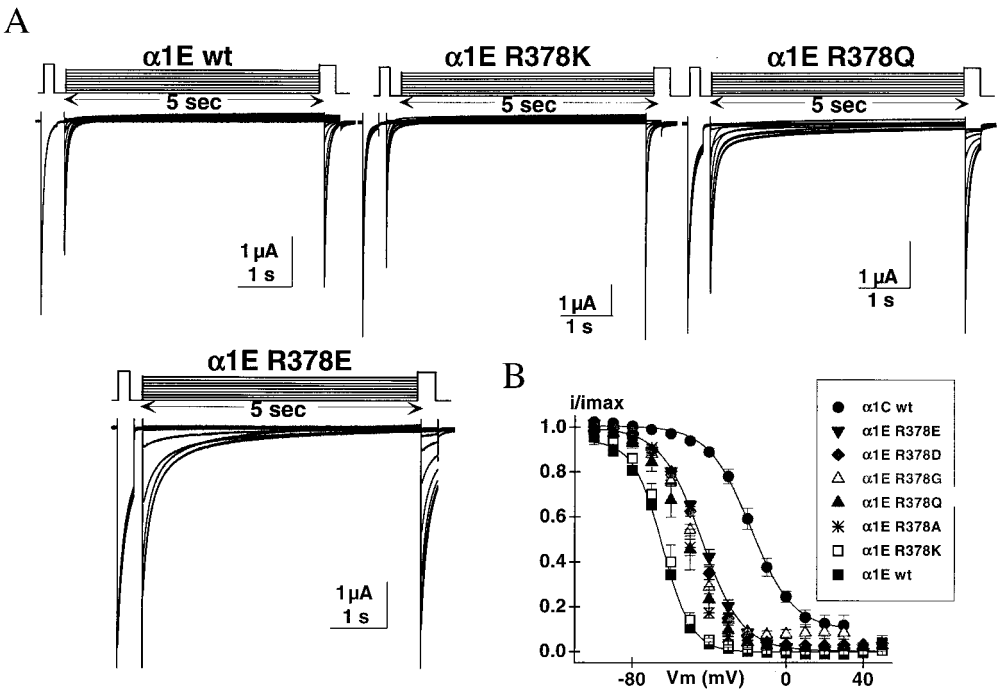

FIGURE 6 (*A*) The voltage dependence of inactivation was estimated from the relative tail currents recorded after a 5-s pulse applied between −100 and +50 mV (10-mV steps). Typical current traces for α1E wt, α1E R378K, α1E R378Q, and α1E R378E are shown from left to right. (*B*) The relative currents were plotted against the prepulse voltage and fitted to the Boltzmann Eq. 1. The estimated mid-potentials of inactivation ($E_{0.5}$) were comparable for α1E wt (■) and for α1E R378K (□) whereas the mid-potentials of inactivation were shifted to the right for α1E R378A (*); α1E R378G (△), α1E R378Q (▲); α1E R378D (◆), and α1E R378E (▼). The voltage dependence of inactivation of the α1C wt (●) channel is shown for comparison. Fit values appear in Table 1.

XWIXXXE. Considering that the I-II linker has recently emerged as an active participant in the inactivation of voltage-dependent calcium channels, we became interested in probing the role of the nonconserved residues in AID through a detailed mutational analysis at this site in α1E. Of the nine nonconserved residues, six positions involving significant changes in charge and/or size, as compared with the same sequence in α1C, were more thoroughly studied: R378E, N381K, R384L, A385D, D388T, K389Q, and K389E. All mutants tested expressed significant whole-cell currents after expression in *Xenopus* oocytes in the presence of α2bδ and β3-subunits. Some of these mutations were studied globally as they were included either in the triple (NRA-KLD), quadruple (NRAK-KLDQ), or the quintuple mutant (NRADK-KLDTQ). Neither multiple mutant displayed significant changes in their kinetics or voltage dependence of inactivation as compared with the wild-type α1E. In contrast, single point mutations of positively charged residues K to E at position K389 and the R to E mutation at position R378 significantly slowed the rate of inactivation. Of the two mutants, only the voltage dependence of inactivation of α1E R378E was affected with ~+20-mV shift in its mid-potential of inactivation as compared with α1E wt. A series of mutations at the R378 position indicated that the net charge carried by the side-chain could play a role in the inactivation kinetics, although the net charge carried by the residue could not explain by itself the effects of R378A, R378G, and R378Q (see below). Alterations in the inactivation properties occurred without any significant difference in the activation properties, hence suggesting that the inactivated state was intrinsically modified by the R378E mutation. The same observation was made for the family of mutants analyzed in this study. However this conclusion regarding the absence of change in the activation potential, remains preliminary in the absence of single-channel data. The relationship between activation and inactivation states cannot be simply overlooked as they are often coupled in voltage-dependent cation channels (Patil et al., 1998).

The reverse mutation E to R in α1C was also shown to speed up inactivation and to shift the voltage dependence of inactivation to more negative membrane potentials (Fig. 7). The rates of α1C E462R and α1E R378E inactivation were both significantly altered and were almost indistinguishable at +20 mV. However, neither point mutation at this position in α1E or α1C channels could completely reverse the inactivation phenotype. Similarly, a series of experiments have shown that the I-II loop from either α1B or α1A produced intermediary inactivation kinetics when inserted into α1E channels but could not completely reverse the inactivation kinetics of α1E (Page et al., 1997). The role of the AID motif in inactivation kinetics has been previously demonstrated in α1A and α1C channels (Herlitze et al., 1997; Sokolov et al., 1999), but this is the first report that the nonconserved R (Arg) residue in the AID motif may contribute to the inactivation phenotype of α1E. Hence, the 5th position of the AID motif could be a universal determinant of inactivation in non-T-type Ca^{2+} channels.

The AID motif has been intensively studied in α1A, α1B, α1C, and α1E channels mostly in terms of its role in G-protein modulation (Toth et al., 1996; Bourinet et al., 1996; Mehrke et al., 1997; Page et al., 1998). Interestingly,

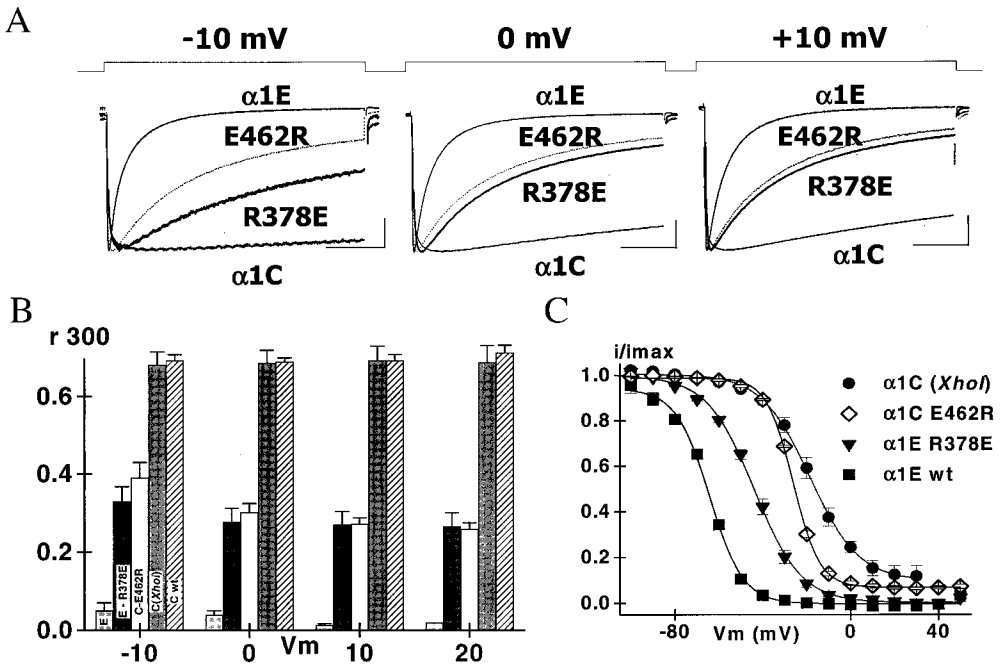

FIGURE 7 (*A*) Whole-cell currents obtained in the presence of 10 mM Ba^{2+} for α1E wt, α1C E462R, α1E R378E, and α1C wt were scaled and superimposed at the voltages of −10 (*left*), 0 (*middle*), and +10 mV (*right*). All α1 subunits were co-injected with α2bδ and β3 subunits. Mutant α1C E462R and α1E R378E inactivated following a time course intermediary between α1E and α1C at all membrane potentials. (*B*) The mean r300 ratios calculated for the same channels are shown ± SEM at four voltages from −10 to +20 mV for α1E wt (*light gray*), α1E R378E (*dark gray*), α1E E462R (*white*), α1C (*XhoI)* (*gray*), and α1C wt (*hatched*) from left to right. The r300 ratios went from 0.05 ± 0.02 at −10 mV and 0.02 ± 0 at +20 mV (n = 17) for α1E, from 0.33 ± 0.04 at −10 mV to 0.27 ± 0.03 at +20 mV (n = 14) for α1E R378E, from 0.39 ± 0.04 at −10 mV to 0.26 ± 0.02 at +20 mV (n = 6) for α1C E462R, from 0.68 ± 0.03 at −10 mV to 0.69 ± 0.04 at +20 mV (n = 6) for α1C (*XhoI*), and from 0.69 ± 0.01 at −10 mV to 0.71 ± 0.02 at +20 mV (n = 9) for α1C wt. (*C*) The voltage dependence of inactivation was estimated from the relative tail currents recorded after 5-s pulses. Normalized currents were fitted to the Boltzmann Eq. 1. The estimated mid-potential of inactivation ($E_{0.5}$) for α1C E462R (◇) was more negative than for the α1C (*XhoI*) construct (●) but more positive than for α1E R378E (▼) and α1E wt (■). The fit values are shown in detail in Table 1.

the R-to-E mutation at the same position of the AID motif has also been shown to eliminate G-protein regulation in α1A (Herlitze et al., 1997). However, it failed to affect G-protein modulation in α1B channels (Zhang et al., 1996) as did the reverse mutation E to R fail to bestow G-protein modulation to α1C channels (Zhang et al., 1996). Despite these small discrepancies, these results suggest that the I-II linker may be specialized to serve as a modulatory domain for Ca^{2+} channel gating with the Arg (R) at position 5 playing a determinant role in many overlapping processes (Zamponi et al., 1997; DeWaard et al., 1997; Herlitze et al., 1997).

A positive residue in the QQXXER motif triggers fast inactivation of α1E (Ca_V2.3)

Only the mutation of the positively charged residue (R378) to negatively charged ones (E or D) at the 5th position of the QQXXER motif affected both the kinetics and voltage dependence of inactivation. Experiments were undertaken to investigate the role of electrostatic interaction in the inactivation kinetics of α1E with additional mutants R378K (positive), R378A (nonpolar and neutral), R378G (polar but neutral), R378Q (polar but neutral), and R378D (negative). At first glance, an electrostatic interaction appears to play a determinant role in the inactivation properties, as α1E R378K was the only mutant to reproduce the wild-type inactivation kinetics and voltage dependence. In contrast, negatively charged mutants R378D and R378E showed the slowest inactivation properties. However, such an interpretation falls short of explaining the behavior of neutral mutants R378A, R378G, and R378Q. Mutant R378A inactivated like R378K between −10 mV and +20 mV. R378Q displayed intermediary inactivation kinetics at −10 mV but tended to inactivate like R378K at +20 mV. R378G produced, on the other hand, slow inactivation kinetics comparable to R378D and R378E at all membrane potentials. Hence, there was no simple correlation between the inactivation kinetics of R378 mutants (R378E, R378D, R378K, R378A, R378Q, and R378G) and any single physicochemical property (charge, polarity, hydropathicity, and hydrophilicity). The intermediary behavior of R378Q could be partly explained by the relative polarity of its side-chain as compared with R378A. However, R378G, which also bears a neutral but slightly polar residue at the same position, diverged from that prediction. Glycine residues are known

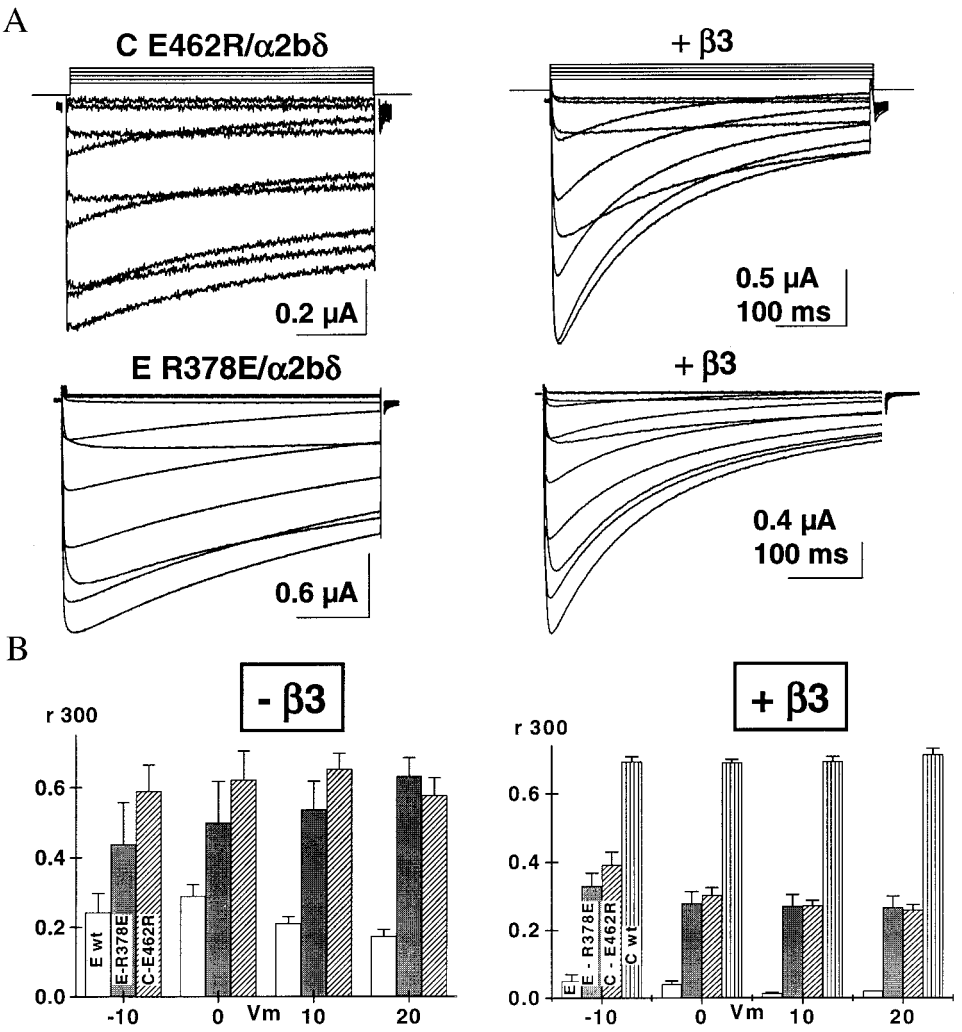

FIGURE 8 β3-Subunit modulation of mutants α1E R378E and α1C E462R. (*A*) The α1E R378E and α1C E462R mutants were expressed in *Xenopus* oocytes in the presence of α2bδ (*left*) and α2bδ/β3 subunits (*right*). Whole-cell currents were recorded with 10 mM Ba^{2+} using a series of pulses from −40 mV to +60 mV from a holding potential of −80 mV. Whole-cell currents peaked at +10 ± 1 mV ($n = 4$) for α1C E462R/α2bδ and +1 ± 1 mV ($n = 7$) for α1C E462R/α2bδ/β3, at +10 ± 1 mV ($n = 3$) for α1E R378E/α2bδ, and at 0 ± 0.2 mV ($n = 3$) for α1E R378E/α2bδ/β3. In both cases, co-injection with the β3-subunit led to a significant increase in their respective inactivation kinetics. Time scale is 100 ms throughout. (*B*) At +10 mV, r300 went from 0.21 ± 0.02 for α1E/α2bδ ($n = 3$) to 0.01 ± 0.005 for α1E/α2bδ/β3 ($n = 6$), from 0.54 ± 0.08 for α1E R378E/α2bδ ($n = 3$) to 0.27 ± 0.03 for α1E R378E/α2bδ/β3 ($n = 9$), and from 0.65 ± 0.05 for α1C E462R/α2bδ ($n = 4$) to 0.27 ± 0.02 for α1C E462R/α2bδ/β3 ($n = 6$).

to confer flexibility to polypeptides (Creighton, 1993), which could considerably lessen whatever interaction takes place at this position. Although sometimes classified with alanine in terms of its physicochemical properties, glycine mutants have been shown to behave distinctively from alanine mutants when introduced into membrane proteins. For instance, in an extensive mutagenesis study of the α1-subunit of the human glycine receptor, Gly mutants at position 288 were found to display EC_{50} similar to the Glu mutants and significantly lower than the wild-type channel with an Ala residue at this position (Yamakura et al., 1999).

Mutations at the fifth position of the AID motif did not prevent β-subunit modulation

The AID motif appears to be cumulating critical determinants for Ca^{2+} channel gating (Herlitze et al., 1997; Dolphin, 1998), namely, in the context of this work (Walker and DeWaard, 1998), voltage-dependent inactivation and β-subunit modulation. Although it had been previously reported that the QQXER motif could play a role in voltage-dependent inactivation, few groups have addressed the possibility that a modification in β-subunit modulation could explain the altered inactivation properties as the mutation involved a residue considered noncritical for β-subunit binding. By investigating the inactivation properties of α1E R378E and α1C E462R in the presence and in the absence of β3, we showed that the R-to-E mutation at the nonconserved position 5 of the AID motif failed to prevent β-subunit modulation. Both mutants displayed the typical hallmarks of β-subunit modulation in Ca^{2+} channels, namely, the increase in peak currents, negative shifts in the voltage dependence of activation and inactivation, and increases in the inactivation kinetics (Fig. 8). These data hence confirmed that the changes in the inactivation kinetics observed in α1E R378E and α1C E462R were intrinsically determined by changes in the α1-subunit. We, however, cannot completely rule out the possibility that mutations within the AID motif could somewhat modify the protein-protein interaction between the mutated α1- and the β-subunits, for modulation and protein interaction could be distinct processes. It is thus possible that β-subunits could modulate the α1-subunit

independently of their ability to bind to the main AID (Yamaguchi et al., 1998). This distinction appears confirmed by a recent study that showed that mutations of the conserved Y (Tyr) residue in α1C (Y467S) had no significant effect on β-subunit-induced modulation of whole-cell currents (Gerster et al., 1999).

Could a hinged-lid mechanism explain voltage-dependent inactivation in Ca^{2+} channels?

It is increasingly suggested that the I-II linker of HVA α1-subunits could behave as an inactivating blocking particle in channels (Bourinet et al., 1999; Cens et al., 1999; Stotz et al., 2000) by analogy to the hinged-lid mechanism described in Na^+ channels. In this scheme, there could be a role for R378 contributing to a conformational change that could eventually cause occlusion of the channel pore. The proposition that inactivation in α1E channels involves the I-II linker as the inactivation gate remains, however, premature at this point in the absence of a three-dimensional structure.

Our data support a major contribution of R378 to the inactivation properties (kinetics and voltage dependence) of α1E. The mutation of a neighboring positive residue in K389E slowed the inactivation kinetics but failed to significantly influence the voltage dependence of inactivation. It remains to be seen, however, whether mutations at this site reverberate on other sites, critical for inactivation, that were not studied in this work. Indeed, mutations at the R378 position failed to completely eliminate voltage-dependent inactivation, indicating that other loci are required to fully account for voltage-dependent inactivation in α1E channels. Some other contributing sites could include, but are not restricted to, residues located downstream to the AID motif or residues located in the C-terminus. Indeed, splice variants in the I-II linker produced α1A channels with altered inactivation phenotypes (Bourinet et al., 1999), and mutations in the C-terminus were shown to slow voltage-dependent inactivation (Bernatchez et al., 1998). By analogy with inactivation in Na^+ and K^+ channels, it is highly possible that sites responsible for voltage-dependent inactivation in the α1E Ca^{2+} channel are distributed along its primary structure.

Our data on the molecular determinants of inactivation in α1E Ca^{2+} channel inactivation highlight some critical differences with the mechanism of fast inactivation in brain Na^+ channels. Point mutations in the I-II linker failed to affect the voltage dependence of activation and inactivation of brain Na^+ channels (Li et al., 1992). Furthermore, charge neutralization in the III-IV linker of the brain Na^+ channel was not found to affect its fast inactivation kinetics (Patton et al., 1992). The locus of inactivation in brain Na^+ channels is composed of three hydrophobic residues, the IFM motif (West et al., 1992). In an extensive site-directed mutagenesis of the Phe (F) site, Catterall and colleagues have shown that normal inactivation kinetics in Na^+ channels requires hydrophobic residues (Kellenberger et al., 1997). In other words, amino acids with aliphatic and aromatic side-chains stabilized the interaction with the putative inactivation receptor activated state whereas hydrophilic ones tended to disrupt it (Kellenberger et al., 1997). Our data suggest that the inactivated state in α1E Ca^{2+} channels could be disrupted by the presence of a negatively charged residue at position R378. Moreover, positively charged residues at position R378 are required to yield the fastest inactivation kinetics whereas nonpolar residues could mimic to a certain extent the normal inactivation kinetics. As the residues in the inactivation ball in the N-terminus of the *Shaker* K^+ channels were mostly hydrophobic (Hoshi et al., 1991), it appears that the molecular mechanisms explaining inactivation in α1E channels could differ substantially from the ones in Na^+ and K^+ channels, especially regarding the nature of the interaction at the inactivation site. It is, in addition, too early to draw any parallel between the observation that inactivation in α1A, α1B, and α1E Ca^{2+} channels could occur from intermediate closed states (Patil et al., 1998) and the general description of voltage-dependent inactivation in many voltage-gated sodium (Armstrong and Bezanilla, 1977; Bean, 1981; Kuo and Bean, 1994) and potassium channels (Hoshi et al., 1990; Demo and Yellen, 1991) where inactivation rates accelerate sharply and progressively in proximity to the open state.

The ongoing debate regarding the molecular locus of voltage-induced inactivation in Ca^{2+} channels underscores the intricate and complex nature of this mechanism. Recent data gathered from mutagenesis studies appear to converge toward residues within the I-II linker in α1E (Stotz et al., 2000; our data), α1C (Herlitze et al., 1997; our data), and α1A channels (Ellinor et al., 1993; Herlitze et al., 1997; Bourinet et al., 1999). As the I-II linker of T-type α1G, α1H, and α1I does not display a high degree of homology with other α1-subunits, transitions to the inactivated state in these channels probably involve other molecular determinants.

We thank Dr. Toni Schneider for the human α1E-subunit, Dr. Ed Perez-Reyes for the β_3-subunit, and Dr. R. Sauvé for critical reading. L.P. is a senior scholar from the Fonds de la Recherche en Santé du Québec.
This work was completed with grants from the Medical Research Council of Canada (MT13390) and from the Canadian Heart and Stroke Foundation to L.P.

REFERENCES

Adams, B., and T. Tanabe. 1997. Structural regions of the cardiac Ca^{2+} channel α_1 subunit involved in Ca^{2+}-dependent inactivation. *J. Gen. Physiol.* 110:379–389.

Armstrong, C. M., and F. Bezanilla. 1977. Inactivation of the sodium channel. II. Gating current experiments. *J. Gen. Physiol.* 70:567–590.

Bean, B. P. 1981. Sodium channel inactivation in the crayfish giant axon: must channels open before inactivating? *Biophys. J.* 35:595–614.

Bernatchez, G., D. Talwar, and L. Parent. 1998. Mutations in the EF-hand motif of the cardiac α_{1C} calcium channel impair the inactivation of barium currents. *Biophys. J.* 75:1727–1739.

Bichet, D., V. Cornet, S. Geib, E. Carlier, S. Volsen, T. Hoshi, Y. Mori, and M. DeWaard. 2000. The I-II loop of the Ca^{2+} channel $\alpha 1$ subunit contains an endoplasmic reticulum retention signal antagonized by the β subunit. *Neuron.* 25:177–190.

Bourinet, E., T. W. Soong, A. Stea, and T. P. Snutch. 1996. Determinants of the G protein-dependent opioid modulation of neuronal calcium channels. *Proc. Natl. Acad. Sci. U.S.A.* 93:1486–1491.

Bourinet, E., T. W. Soong, K. Sutton, S. Slaymaker, E. Mathews, A. Monteil, G. W. Zamponi, J. Nargeot, and T. P. Snutch. 1999. Splicing of $\alpha 1$A subunit gene generates phenotypic variants of P- and Q-type calcium channels. *Nat. Neurosci.* 2:407–415.

Campbell, V., N. S. Berrow, E. M. Fitzgerald, K. Brickley, and A. C. Dolphin. 1995. Inhibition of the interaction of G protein G(o) with calcium channels by the calcium channel β subunit in rat neurones. *J. Physiol. (Lond.).* 485:365–372.

Castellano, A., X. Wei, L. Birnbaumer, and E. Perez-Reyes. 1993. Cloning and expression of a third calcium channel β subunit. *J. Biol. Chem.* 268:3450–3455.

Cens, T., S. Restituito, S. Galas, and P. Charnet. 1999. Voltage and calcium use the same molecular determinants to inactivate calcium channels. *J. Biol. Chem.* 274:5483–5490.

Creighton, T. E. 1993. Proteins, Structure and Molecular Properties. W. H. Freeman, New York.

Cribbs, L. L., J. C. Gomora, A. N. Daud, J. H. Lee, and E. Perez-Reyes. 2000. Molecular cloning and functional expression of Ca(v)3.1c, a T-type calcium channel from human brain. *FEBS Lett.* 466:54–58.

Cribbs, L. L., J. H. Lee, J. Yang, J. Satin, Y. Zhang, A. Daud, J. Barclay, M. P. Williamson, M. Fox, M. Rees, and E. Perez-Reyes. 1998. Cloning and characterization of $\alpha 1$H from human heart, a member of the T-type Ca^{2+} channel gene family. *Circ. Res.* 83:103–109.

deLeon, M., Y. Wang, L. Jones, E. Perez-Reyes, X. Wei, T. W. Soong, T. P. Snutch, and D. T. Yue. 1995. Essential Ca^{2+}-binding motif for Ca^{2+}-sensitive inactivation of L-type Ca^{2+} channels. *Science.* 270: 1502–1506.

Demo, S. D., and G. Yellen. 1991. The inactivation gate of the *Shaker* K^+ channel behaves like an open-channel blocker. *Neuron.* 7:743–753.

Deng, W. P., and J. A. Nickoloff. 1992. Site-directed mutagenesis of virtually any plasmid by eliminating a unique site. *Anal. Biochem.* 200:81–88.

DeWaard, M., and K. P. Campbell. 1995. Subunit regulation of the neuronal α_{1A} Ca^{2+} channel expressed in *Xenopus* oocytes. *J. Physiol. (Lond.).* 485:619–634.

DeWaard, M., H. Liu, D. Walker, V. E. Scott, C. A. Gurnett, and K. P. Campbell. 1997. Direct binding of G-protein $\beta\gamma$ complex to voltage-dependent calcium channels. *Nature.* 385:446–500.

DeWaard, M., V. E. Scott, M. Pragnell, and K. P. Campbell. 1996. Identification of critical amino acids involved in α_1-β interaction in voltage-dependent Ca^{2+} channels. *FEBS Lett.* 380:272–276.

Dolphin, A. C. 1998. Mechanisms of modulation of voltage-dependent calcium channels by G proteins. *J. Physiol.* 506:3–11.

Ellinor, P. T., J. F. Zhang, A. D. Randall, M. Zhou, T. L. Schwarz, R. W. Tsien, and W. A. Horne. 1993. Functional expression of a rapidly inactivating neuronal calcium channel. *Nature.* 363:455–458.

Ertel, E. A., K. P. Campbell, M. M. Harpold, F. Hofmann, Y. Mori, E. Perez-Reyes, A. Schwartz, T. P. Snutch, T. Tanabe, L. Birnbaumer, R. W. Tsien, and W. A. Catterall. 2000. Nomenclature of voltage-gated calcium channels. *Neuron.* 25:533–535.

Gerster, U., B. Neuhuber, K. Groschner, J. Striessnig, and B. E. Flucher. 1999. Current modulation and membrane targeting of the calcium channel $\alpha 1$C subunit are independent functions of the β subunit. *J. Physiol. (Lond.).* 517:353–368.

Herlitze, S., G. H. Hockerman, T. Scheuer, and W. A. Catterall. 1997. Molecular determinants of inactivation and G protein modulation in the intracellular loop connecting domains I and II of the calcium channel α_{1A} subunit. *Proc. Natl. Acad. Sci. U.S.A.* 94:1512–1516.

Hoshi, T., W. N. Zagotta, and R. W. Aldrich. 1990. Biophysical and molecular mechanisms of *Shaker* potassium channel inactivation. *Science.* 250:533–538.

Hoshi, T., W. N. Zagotta, and R. W. Aldrich. 1991. Two types of inactivation in *Shaker* K^+ channels: effects of alterations in the carboxy-terminal region. *Neuron.* 7:547–556.

Kellenberger, S., J. W. West, T. Scheuer, and W. A. Catterall. 1997. Molecular analysis of the putative inactivation particle in the inactivation gate of brain type IIA Na^+ channels. *J. Gen. Physiol.* 109:589–605.

Kuo, C. C., and B. P. Bean. 1994. Na^+ channels must deactivate to recover from inactivation. *Neuron.* 12:819–829.

Lacerda, A. E., E. Perez-Reyes, X. Wei, A. Castellano, and A. M. Brown. 1994. T-type and N-type calcium channels of *Xenopus* oocytes: evidence for specific interactions with β subunits. *Biophys. J.* 66:1833–1843.

Lee, J. H., A. N. Daud, L. L. Cribbs, A. E. Lacerda, A. Pereverzev, U. Klockner, T. Schneider, and E. Perez-Reyes. 1999a. Cloning and expression of a novel member of the low voltage-activated T-type calcium channel family. *J. Neurosci.* 19:1912–1921.

Lee, A., S. T. Wong, D. Gallagher, B. Li, D. R. Storm, T. Scheuer, and W. A. Catterall. 1999b. Ca^{2+}/calmodulin binds to and modulates P/Q-type calcium channels. *Nature.* 399:155–159.

Li, M., J. W. West, Y. Lai, T. Scheuer, and W. A. Catterall. 1992. Functional modulation of brain sodium channels by cAMP-dependent phosphorylation. *Neuron.* 8:1151–1159.

Mehrke, G., A. Pereverzev, H. Grabsch, J. Hescheler, and T. Schneider. 1997. Receptor-mediated modulation of recombinant neuronal class E calcium channels. *FEBS Lett.* 408:261–270.

Monteil, A., J. Chemin, E. Bourinet, G. Mennessier, P. Lory, and J. Nargeot. 2000. Molecular and functional properties of the human $\alpha 1$G subunit that forms T-type calcium channels. *J. Biol. Chem.* 275: 6090–6100.

Page, K. M., C. Canti, G. J. Stephens, N. S. Berrow, and A. C. Dolphin. 1998. Identification of the amino terminus of neuronal Ca^{2+} channel α_1 subunits α_{1B} and α_{1E} as an essential determinant of G-protein modulation. *J. Neurosci.* 18:4815–4824.

Page, K. M., G. J. Stephens, N. S. Berrow, and A. C. Dolphin. 1997. The intracellular loop between domains I and II of the B-type calcium channel confers aspects of G-protein sensitivity to the E-type calcium channel. *J. Neurosci.* 17:1330–1338.

Parent, L., and M. Gopalakrishnan. 1995. Glutamate substitution in repeat IV alters divalent and monovalent cation permeation in the heart Ca^{2+} channel. *Biophys. J.* 69:1801–1813.

Parent, L., M. Gopalakrishnan, A. E. Lacerda, X. Wei, and E. Perez-Reyes. 1995. Voltage-dependent inactivation in a cardiac-skeletal chimeric calcium channel. *FEBS Lett.* 360:144–150.

Parent, L., T. Schneider, C. P. Moore, and D. Talwar. 1997. Subunit regulation of the humain brain α_{1E} calcium channel. *J. Membr. Biol.* 160:127–140.

Patil, P. G., D. L. Brody, and D. T. Yue. 1998. Preferential closed-state inactivation of neuronal calcium channels. *Neuron.* 20:1027–1038.

Patton, D. E., J. W. West, W. A. Catterall, and A. L. Goldin. 1992. Amino acid residues required for fast Na^+ channel inactivation: charge neutralizations and deletions in the III-IV linker. *Proc. Natl. Acad. Sci. U.S.A.* 89:10905–10909.

Perez-Reyes, E., L. L. Cribbs, A. Daud, A. E. Lacerda, J. Barclay, M. P. Williamson, M. Fox, M. Rees, and J. H. Lee. 1998. Molecular characterization of a neuronal low-voltage-activated T-type calcium channel. *Nature.* 391:896–900.

Peterson, B. Z., C. D. DeMaria, J. P. Adelman, and D. T. Yue. 1999. Calmodulin is the Ca^{2+} sensor for Ca^{2+}-dependent inactivation of L-type calcium channels. *Neuron.* 22:549–558.

Peterson, B. Z., J. S. Lee, J. G. Mulle, Y. Wang, L. M. de, and D. T. Yue. 2000. Critical determinants of Ca^{2+}-dependent inactivation within an EF-hand motif of L-type Ca^{2+} channels. *Biophys. J.* 78:1906–1920.

Piedras-Renteria, E. S., and R. W. Tsien. 1998. Antisense oligonucleotides against α_{1E} reduce R-type calcium currents in calcium currents in cerebellar granule cells. *Proc. Natl. Acad. Sci. U.S.A.* 95:7760–7765.

Pragnell, M., M. De Waard, Y. Mori, T. Tanabe, T. P. Snutch, and K. P. Campbell. 1994. Calcium channel β-subunit binds to a conserved motif in the I-II cytoplasmic linker of the α_1-subunit. *Nature.* 368:67–70.

Qin, N., R. Olcese, M. Bransby, T. Lin, and L. Birnbaumer. 1999. Ca^{2+}-induced inhibition of the cardiac Ca^{2+} channel depends on calmodulin. *Proc. Natl. Acad. Sci. U.S.A.* 96:2435–2438.

Randall, A. D., and R. W. Tsien. 1997. Contrasting biophysical and pharmacological properties of T-type and R-type calcium channels. *Neuropharmacology.* 36:879–893.

Saegusa, H., T. Kurihara, S. Zong, O. Minowa, A. Kazuno, W. Han, Y. Matsuda, H. Yamanaka, M. Osanai, T. Noda, and T. Tanabe. 2000. Altered pain responses in mice lacking α1E subunit of the voltage-dependent Ca^{2+} channel. *Proc. Natl. Acad. Sci. U.S.A.* 97:6132–6137.

Sambrook, J., E. F. Fritsch, and T. Maniatis. 1989. Molecular Cloning: A Laboratory Manual, 2nd ed. Cold Spring Harbor Laboratory Press, Cold Spring Harbor, NY.

Sokolov, S., R. G. Weiss, B. Kurka, F. Gapp, and S. Hering. 1999. Inactivation determinant in the I-II loop of the Ca^{2+} channel α1-subunit and β-subunit interaction affect sensitivity for the phenylalkylamine (−)gallopamil. *J. Physiol. (Lond.).* 519:315–322.

Stephens, G. J., K. M. Page, Y. Bogdanov, and A. C. Dolphin. 2000. The α1B Ca^{2+} channel amino terminus contributes determinants for subunit-mediated voltage-dependent inactivation properties. *J. Physiol. (Lond.).* 525:377–390.

Stotz, S. C., J. Hamid, R. L. Spaetgens, S. E. Jarvis, and G. W. Zamponi. 2000. Fast inactivation of voltage-dependent calcium channels: a hinged-lid mechanism. *J. Biol. Chem.* 275:24575–24582.

Tareilus, E., M. Roux, N. Qin, R. Olcese, J. Zhou, E. Stefani, and L. Birnbaumer. 1997. A *Xenopus* oocyte β subunit: evidence for a role in the assembly/expression of voltage-gated calcium channels that is separate from its role as a regulatory subunit. *Proc. Natl. Acad. Sci. U.S.A.* 94:1703–1708.

Toth, P. T., L. R. Shekter, G. H. Ma, L. H. Philipson, and R. J. Miller. 1996. Selective G-protein regulation of neuronal calcium channels. *J. Neurosci.* 16:4617–4624.

Walker, D., D. Bichet, S. Geib, E. Mori, V. Cornet, T. P. Snutch, Y. Mori, and M. De Waard. 1999. A new β subtype-specific interaction in α1A subunit controls P/Q-type Ca^{2+} channel activation. *J. Biol. Chem.* 274: 12383–12390.

Walker, D., and M. De Waard. 1998. Subunit interaction sites in voltage-dependent Ca^{2+} channels: role in channel function. *Trends Neurosci.* 21:148–154.

West, J. W., D. E. Patton, T. Scheuer, Y. Wang, A. L. Goldin, and W. A. Catterall. 1992. A cluster of hydrophobic amino acid residues required for fast Na^{+} channel inactivation. *Proc. Natl. Acad. Sci. U.S.A.* 89: 10910–10914.

Williams, M. E., D. H. Feldman, A. F. McCue, R. Brenner, G. Velicelebi, S. B. Ellis, and M. M. Harpold. 1992. Structure and functional expression of α_1, α_2, and β subunits of a novel human neuronal calcium channel subtype. *Neuron.* 8:71–84.

Yamaguchi, H., M. Hara, M. Strobeck, K. Fukasawa, A. Schwartz, and G. Varadi. 1998. Multiple modulation pathways of calcium channel activity by a β subunit: direct evidence of β subunit participation in membrane trafficking of the α1C subunit. *J. Biol. Chem.* 273:19348–19356.

Yamakura, T., S. J. Mihic, and R. A. Harris. 1999. Amino acid volume and hydropathy of a transmembrane site determine glycine and anesthetic sensitivity of glycine receptors. *J. Biol. Chem.* 274:23006–23012.

Zamponi, G. W., E. Bourinet, D. Nelson, J. Nargeot, and T. P. Snutch. 1997. Crosstalk between G proteins and protein kinase C mediated by the calcium channel α1 subunit. *Nature.* 385:442–446.

Zhang, J. F., P. T. Ellinor, R. W. Aldrich, and R. W. Tsien. 1996. Multiple structural elements in voltage-dependent Ca^{2+} channels support their inhibition by G proteins. *Neuron.* 17:991–1003.

Zhou, J., R. Olcese, N. Qin, F. Noceti, L. Birnbaumer, and E. Stefani. 1997. Feedback inhibition of Ca^{2+} channels by Ca^{2+} depends on a short sequence of the C terminus that does not include the Ca^{2+}-binding function of a motif with similarity to Ca^{2+}-binding domains. *Proc. Natl. Acad. Sci. U.S.A.* 94:2301–2305.

Zuhlke, R. D., G. S. Pitt, K. Deisseroth, R. W. Tsien, and H. Reuter. 1999. Calmodulin supports both inactivation and facilitation of L-type calcium channels. *Nature.* 399:159–162.